

Robust RL with LLM-Driven Data Synthesis and Policy Adaptation for Autonomous Driving

Sihao Wu^{1*}, Jiaxu Liu^{1*}, Xiangyu Yin¹, Guangliang Cheng¹, Xingyu Zhao²,
Meng Fang¹, Xinpeng Yi³, Xiaowei Huang¹

¹University of Liverpool, ²WMG, University of Warwick, ³Southeast University
{firstname.lastname}@liverpool.ac.uk, xingyu.zhao@warwick.ac.uk, xyi@seu.edu.cn

Abstract: The integration of Large Language Models (LLMs) into autonomous driving systems demonstrates strong common sense and reasoning abilities, effectively addressing the pitfalls of purely data-driven methods. Current LLM-based agents require lengthy inference times and face challenges in interacting with real-time autonomous driving environments. A key open question is whether we can effectively leverage the knowledge from LLMs to train an efficient and robust Reinforcement Learning (RL) agent. This paper introduces RAPID, a novel **Robust Adaptive Policy Infusion and Distillation** framework, which trains specialized mix-of-policy RL agents using data synthesized by an LLM-based driving agent and online adaptation. RAPID features three key designs: 1) utilization of offline data collected from an LLM agent to distil expert knowledge into RL policies for faster real-time inference; 2) introduction of robust distillation in RL to inherit both performance and robustness from LLM-based teacher; and 3) employment of a mix-of-policy approach for joint decision decoding with a policy adapter. Through fine-tuning via online environment interaction, RAPID reduces the forgetting of LLM knowledge while maintaining adaptability to different tasks. Extensive experiments demonstrate RAPID’s capability to effectively integrate LLM knowledge into scaled-down RL policies in an efficient, adaptable, and robust way. Code and checkpoints will be made publicly available upon acceptance.

Keywords: Reinforcement Learning, Robust Knowledge Distillation, LLM

1 Introduction

The integration of Large Language Models (LLMs) with emergent capabilities into autonomous driving presents an innovative approach [1, 2, 3]. Previous work suggests that LLM can significantly enhance the common sense and reasoning abilities of autonomous vehicles, effectively addressing several pitfalls of purely data-driven methods [4, 5, 6]. However, LLMs face several challenges, primarily in generating effective end-to-end instructions in real-time and dynamic driving scenarios. This limitation stems from two primary factors: the extended inference time required by LLM-based agents [5] and the difficulty these agents face in continuous data collection and learning [7], which renders them unsuitable for real-time decision-making in dynamic driving environments. Furthermore, faster and smaller models, which are often preferred for real-time applications, have a higher risk of being vulnerable to adversarial attacks compared to larger models [8, 9, 10, 11]. These challenges drive us to tackle the following questions:

How to develop an **efficient**, **adaptable**, and **robust** agent that can leverage the capabilities of the LLM-based agent for autonomous driving?

One potential solution is to use the LLM as a teacher policy to instruct the learning of a lighter, specialized student RL policy through knowledge distillation [12, 13]. This allows the student model to inherit the reasoning abilities of the LLM while being lightweight enough for real-time infer-

ence. Another approach is to employ LLMs to generate high-level plans or instructions, which are then executed by a separate controller [14]. This decouples the reasoning and execution processes, allowing for faster reaction times. Furthermore, techniques such as Instruction Tuning (IT) [15] and In-Context Learning (ICL) [16] can adapt the LLM to new tasks without extensive fine-tuning. However, these approaches still have limitations. Knowledge distillation may result in information forgetting or loss of generalization ability. Generating high-level plans relies on the strong assumption that the LLM can provide complete and accurate instructions. IT and ICL are sensitive to the choice of prompts and demonstrations, which require careful design for each task [17, 18].

To tackle the above challenges, we propose RAPID, a **R**obust **A**ddaptive **P**olicy **I**nfusion and **D**istillation framework that incorporates LLM knowledge into offline RL for autonomous driving, to leverage the common sense and robust ability of LLM and solve challenging scenarios such as unseen corner cases. Our method encompasses several designs: (1) We utilize offline data collected from LLMs-based agents to facilitate the distillation of expertise information into faster policies for real-time inference. (2) We introduce robust distillation in offline RL to inherit not only performance but also the robustness from LLM teachers. (3) We introduce mix-of-policy for joint action decoding with policy adapter. Through fine-tuning via online environment interaction, we prevent the forgetting of LLM knowledge while keeping the adaptability to various RL environments.

To the best of our knowledge, this work pioneers the distillation of knowledge from LLM-based agents into RL policies through offline training combined with online adaptation in the context of autonomous driving. Through extensive experiments, we demonstrate RAPID’s capability to effectively integrate LLM knowledge into scaled-down RL policies in a transferable, robust, and efficient way.

2 Preliminaries

Notation. We view a sequential decision-making problem, formalized as a Markov Decision Process (MDP), denoted by $\langle \mathcal{S}, \mathcal{A}, \mathcal{T}, \mathcal{R}, \gamma \rangle$, where \mathcal{S} and \mathcal{A} represent the state and action spaces, respectively. The transition probability function is denoted by $\mathcal{T} : \mathcal{S} \times \mathcal{A} \rightarrow \mathcal{P}(\mathcal{S})$, and the reward function is denoted by $\mathcal{R} : \mathcal{S} \times \mathcal{A} \times \mathcal{S} \rightarrow \mathbb{R}$. Moreover, γ denotes the discount factor. The main objective is to acquire an optimal policy, denoted as $\pi : \mathcal{S} \rightarrow \mathcal{A}$, that maximizes the expected cumulative return over time, $\max_{\pi} \mathbb{E}[\sum_t \gamma^t r_t]$. The policy parameter θ , denoted in π , is crucial. A typical gradient-based RL algorithm minimizes a surrogate loss, $J(\theta)$, employing gradient descent concerning θ . This loss is estimated using sampled trajectories, wherein each trajectory comprises a sequence of state-action-reward tuples.

Offline RL. The aim is to learn effective policies from pre-collected datasets, eliminating the need for further interaction. Given a dataset $\mathcal{D} = \{(\mathbf{s}, \mathbf{a}, r, \mathbf{s}')\}$ containing trajectories collected under an unknown behavior policy π_B , the iterative Q update step with learned policy π is expressed as

$$\hat{Q}^{k+1} \leftarrow \arg \min_Q J(Q, \pi, \mathcal{D}), \quad (\text{Policy Evaluation}) \quad (1)$$

$$\text{where } J(Q, \pi, \mathcal{D}) := \mathbb{E}_{\mathbf{s}, \mathbf{a}, \mathbf{s}' \sim \mathcal{D}} \left[\left((r(\mathbf{s}, \mathbf{a}) + \gamma \mathbb{E}_{\mathbf{a}' \sim \hat{\pi}(\mathbf{a}'|\mathbf{s}')} [\hat{Q}^k(\mathbf{s}', \mathbf{a}')]) - Q(\mathbf{s}, \mathbf{a}) \right)^2 \right]. \quad (2)$$

With the updated Q-function, the policy is improved by

$$\hat{\pi}^{k+1} \leftarrow \arg \max_{\pi} \mathbb{E}_{\mathbf{s} \sim \mathcal{D}, \mathbf{a} \sim \pi^k(\mathbf{a}|\mathbf{s})} [\hat{Q}^{k+1}(\mathbf{s}, \mathbf{a})]. \quad (\text{Policy Improvement}) \quad (3)$$

Conservative Q-Learning. Offline RL algorithms following this fundamental approach are often challenged by the issue of action distribution shift [19]. Therefore, [20] proposed conservative Q-learning, where the Q values are penalized by Out-Of-Distribution (OOD) actions

$$\hat{Q}^{k+1} \leftarrow \arg \min_Q J(Q, \pi, \mathcal{D}) + \alpha \left(\mathbb{E}_{\mathbf{s} \sim \mathcal{D}, \mathbf{a} \sim \mu(\cdot|\mathbf{s})} [Q(\mathbf{s}, \mathbf{a})] - \mathbb{E}_{\mathbf{s}, \mathbf{a} \sim \mathcal{D}} [Q(\mathbf{s}, \mathbf{a})] \right), \quad (4)$$

where μ is an approximation of the policy that maximizes the current Q-function. While [21] found that the effectiveness of Offline RL algorithms is significantly influenced by the characteristics of the dataset, which also motivated us to explore the influence of LLM-generated dataset.

3 RAPID: Robust Distillation and Adaptive Policy Infusion

3.1 Offline Dataset Collection

As shown in Fig. 2 (a), we conducted a closed-loop driving experiment on HighwayEnv [22] using GPT-3.5 [23] to collect the offline dataset. The vehicle density and number of lanes in HighwayEnv can be adjusted, and we choose LANE-3-DENSITY-2 as the base environment. As a text-only LLM, GPT-3.5 cannot directly interact with the HighwayEnv simulator. To facilitate its observation and decision-making processes, the experiment incorporated perception tools and agent prompts, enabling GPT-3.5 to effectively engage with the simulated environment. The prompts have the following stages: (1) Prefix prompt: The LLM obtains the current driving scene and historical information. (2) Reasoning: By employing the ReAct framework [24], the LLM-based agent reasons about the appropriate driving actions based on the scene. (3) Output decision: The LLM outputs its decision on which meta-action to take. The agent has access to 5 meta-actions: `lane_left`, `lane_right`, `faster`, `slower`, and `idle`. More details about the prompt setup are instructed in Appendix F. Through an iterative closed-loop process described above, we collect the dataset $\mathcal{D}_{\text{LLM}} = \{(s, a, r, s') | a \sim \pi_{\text{LLM}}(a|s)\}$, where the π_{LLM} is the LLM agent.

3.2 Robustness Regularized Distillation

Recall the offline RL objective in Eq. (3-4). Let the LLM-distil policy be π_{distil} , with the collected dataset \mathcal{D}_{LLM} , the offline training is to optimize $J(Q, \pi_{\text{distil}}, \mathcal{D}_{\text{LLM}})$ for an improved Q function, then update the policy *w.r.t* Q . Empirically as shown in Fig. 1, the LLM-based agent π_{LLM} is more robust against malicious state injection under the autonomous driving setting. However, a distilled offline policy is not as robust compared to LLMs, demonstrated by [25], where the Q value can change drastically over neighbouring states, leading to an unstable policy. Therefore, vanilla offline RL algorithms cannot robustly distil information to the LLM-distil agent. Inspired by [10, 11], we formulate a novel training objective by introducing a discrepancy term into Eq. (4), allowing the distillation of adversarial knowledge to the offline agent.

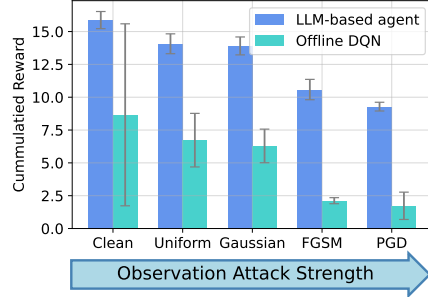


Figure 1: Cumulative reward on LANE-3-DENSITY-2 with progressively increasing observation (s) attack strength. The LLM-based agent π_{LLM} exhibits improved robustness compared with vanilla Offline DQN.

$$J_{\text{robust}}(Q, \pi, \mathcal{D}) := J(Q, \pi, \mathcal{D}) + \alpha (\mathbb{E}_{s \sim \mathcal{D}, a \sim \mu(\cdot|s)} [Q(s, a)] - \mathbb{E}_{s, a \sim \mathcal{D}} [Q(s, a)]) \quad (5)$$

$$+ \beta \left(\mathbb{E}_{s, a \sim \mathcal{D}} \left[\log \left(\frac{\sigma(Q(\tilde{s}, a))}{\text{onehot}(a)} \right) \right] \right), \text{ where } \tilde{s} = \arg \max_{\|\tilde{s} - s\|_2 \leq \epsilon} \mathbb{E}_{s, a \sim \mathcal{D}} \left[\log \left(\frac{\sigma(Q(\tilde{s}, a))}{\text{onehot}(a)} \right) \right].$$

In Eq. (5), $\sigma(\cdot)$ denote the softmax(\cdot) function, characterizing the probability that the Q network will choose each action. $\text{onehot}(\cdot)$ converts the selected action from the offline dataset to a one-hot vector, characterizing the definite events. Therefore, $\mathbb{E}_{s, a \sim \mathcal{D}} \left[\log \left(\frac{\sigma(Q(\tilde{s}, a))}{\text{onehot}(a)} \right) \right]$ can be viewed as the KL divergence between the Q network output distribution and the categorical distribution of one-hot action. Essentially, the $\arg \max$ constraint identifies the adversarial state that yields the worst Q performance, while the objective J_{robust} seeks to find the optimal Q function to neutralize the adversarial attack. This process forms an adversarial training procedure, where α and β are hyperparameters that balance the conservative and robustness terms, respectively.

3.3 LLM Knowledge Infused Robust Policy with Environment Adaptation

In autonomous driving, the RL policy typically has the overview of the ego car, as well as surrounding cars' information. The ego action is predicted by considering the motion of all captured cars. Assuming V vehicles captured, F vehicle features and A action features¹, the state can be

¹features: highway-env.farama.org/observations, actions: highway-env.farama.org/actions

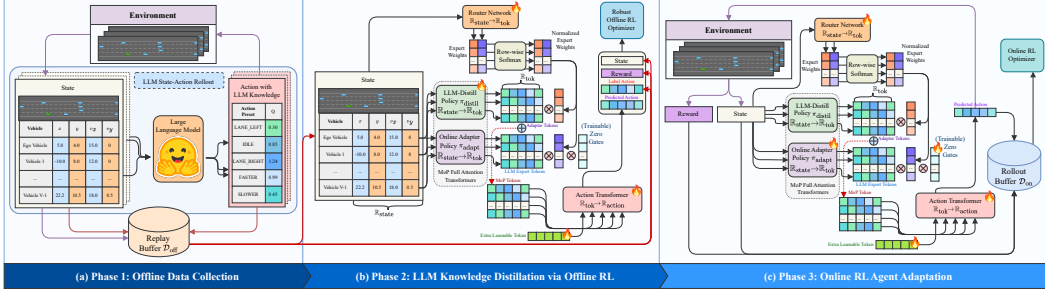



Figure 2: Our proposed RAPID framework. Only modules tagged by  are trained. (a) *Phase 1:* Collect state-action rollouts from an environment and store them in a replay buffer. (b) *Phase 2:* Distill LLM knowledge into an offline policy using the collected data, the adapter policy is frozen and its output tokens are masked by zero gates. (c) *Phase 3:* Adapt the pre-trained model online by interacting with the environment, the LLM-distilled policy is frozen, and the zero gate is trained for progressive adaptation.

encapsulated by a matrix in $\mathbb{R}^{V \times F}$, and the action is simply a vector in \mathbb{R}^A . A typical way to obtain actions from observations is to concat all V features in a row, then feed into a MLP: $\mathbb{R}^{V \times F} \rightarrow \mathbb{R}^A$. However, when the vanilla RL agent is expanded to multi-policy for joint decision, *i.e.*, the action is modelled via interdisciplinary collaboration (*e.g.* *LLM-distilled knowledge & online environment*). In such a case, simple MLPs encode vehicles as one unified embedding, which fails to model the explicit decision process for each other vehicle, thus lacking in explainability. Below, we discuss how to incorporate different sources of knowledge for joint decision prediction.

3.3.1 Mixture-of-Policies via Vehicle Features Tokenization

Let the observation $\mathbf{s} \in \mathbb{R}^{V \times F}$, assume we have N policies for joint decision. Our approach is to revise the state \mathbf{s} as a sequence of tokens, where the sequence is of length V and each token is of dimension F . Borrowing ideas from language models [26, 27, 28], we implement *mixture-of-policies* (MoP) for joint-decision. As detailed below, we illustrate the process to obtain action \mathbf{a} from state \mathbf{s} . Assume the N policies $\pi_{1...N} : \mathbb{R}^{V \times F} \rightarrow \mathbb{R}^{V \times D}$ where D is the latent token dim. The state is first fed into a router network $G : \mathbb{R}^{V \times F} \rightarrow \mathbb{R}^{V \times N}$ to get the policy weights $G(\mathbf{s}) \in \mathbb{R}^{V \times N}$. Then a topK and Softmax is applied column-wise to select the most influential K policies and get the normalization $\omega = \text{softmax}(\text{topK}(G(\mathbf{s}))) \in \mathbb{R}^{V \times N}$. Next, we calculate output sequences of all policies: $\mathbf{t} = \{\pi_i(\mathbf{s})\}_{i=1}^N \in \mathbb{R}^{N \times V \times D}$. The mixed policy is then the weighted mean of sequences, expressed as $\tilde{\mathbf{a}} = \sum_{i=1}^N (\omega^\top)_i \cdot \mathbf{t}_i \in \mathbb{R}^{V \times D}$. Finally the action is obtained via action decoder $\text{dec} : \mathbb{R}^{V \times D} \rightarrow \mathbb{R}^A$. In one equation, the joint policy $\mathbf{s} \rightarrow \mathbf{a}$ is formulated by

$$\mathbf{a} = \Pi_{\text{MoP}}(\mathbf{s}; \theta_d, \theta_r, \theta_p) := \text{dec}_{\theta_d} \left(\sum_{i=1}^N \left[\left([\text{softmax}(\text{topK}(G_{\theta_r}(\mathbf{s})))^\top]_i \cdot \pi_i(\mathbf{s}; \theta_p^{(i)}) \right) \right] \right) \quad (6)$$

where $\theta_d, \theta_r, \theta_p$ are respectively the parameters of action decoder, router, and policies. Π_{MoP} represents the mixed policy for the joint decision from both distilled policy and online adaptation policy. In practice, we design the policies as full-attention transformers, and decoder dec_{θ_d} as a ViT-wise transformer, taking $1 + V$ tokens as input sequence where the first token is an extra learnable token. The extra token's embedding is decoded as the predicted action. For detailed implementation of MoP policies and the action decoder, please refer to Appendix C.

Remark 1. One simple alternative to joint action prediction is to mix actions instead of policies. Regarding N policies as $\text{mlp}_{1...N} : \mathbb{R}^{V \times F} \rightarrow \mathbb{R}^A$, the final action $\mathbf{a} \in \mathbb{R}^A$ is then the merge of their respective decisions, *i.e.* $\mathbf{a} = \text{merge}(\text{mlp}_{1...N}(\text{flat}(\mathbf{s})); w_{1...N})$ where $\text{flat} : \mathbb{R}^{V \times F} \rightarrow \mathbb{R}^{V \times F}$. However, this approach presents several problems: **Q1:** Weights $w_{1...N}$, despite learnable, are fixed vehicle-wise. This means all vehicles in policy 1 share the same w_1 for action prediction, same as for other policies. **Q2:** Weights are independent of observations, which are not generalizable

to constantly varying environments. **Q3**: The merge is not a sparse selection, meaning all policy candidates are selected for action decision, resulting in loss of computational efficiency when N increases. Using Eq. (6), as $\omega^\top \in \mathbb{R}^{N \times V}$, for each policy, we have V different weights for each vehicle, this resolves **Q1**. Meanwhile, as ω is generated from routed state $G(s)$, which is adaptive to varying states, this resolves **Q2**. **Q3** is also resolved through employing topK, when $K < N$, the selection on policies will be sparse.

3.3.2 Online Adaptation to Offline Policy with Mixture-of-Policies

Our employment of Eq. (6) is illustrated in Fig. 2, a special case where $N = K = 2$. The policies come from two sources, respectively, the distilled language model knowledge (*LLM-distill Policy*, $\pi_1 = \pi_{\text{distil}}$) and the online environment interaction (*Online Adapter Policy*, $\pi_2 = \pi_{\text{adapt}}$). The robust distillation principal (Eq. (5)) is integrated into the offline distillation phase (Fig. 2.(b)). Respectively, the objective for Q-network & joint policy update is expressed as

$$\hat{Q}^{k+1} \leftarrow \arg \min_Q J_{\text{robust}}(Q, \Pi_{\text{MoP}}(\cdot; \theta_d, \theta_r, \theta_p), \mathcal{D}_{\text{off}}), \text{ (Robust Offline Q-Learning)} \quad (7)$$

$$\hat{\Pi}_{\text{MoP}}^{k+1} \leftarrow \arg \max_{\theta_d, \theta_r, \theta_p^{(1)}} \mathbb{E}_{\mathbf{s} \sim \mathcal{D}_{\text{off}}, \mathbf{a} \sim \Pi_{\text{MoP}}^k(\cdot; \mathbf{s}; \theta_d, \theta_r, \theta_p)} [\hat{Q}^{k+1}(\mathbf{s}, \mathbf{a})]. \text{ (LLM Policy Improvement)} \quad (8)$$

The parameters $\theta_p^{(2)}$ of π_2 (π_{adapt}) during policy improvement (Eq. (8)) are frozen since LLM knowledge should only be distilled into π_1 (π_{distil}). With an arbitrary RL algorithm, the online adaptation phase objective can be expressed by

$$\hat{\Pi}_{\text{MoP}}^* = \arg \max_{\theta_d, \theta_r, \theta_p^{(2)}} \mathbb{E}_{\mathbf{s} \sim \mathcal{D}_{\text{on}}, \mathbf{a} \sim \Pi_{\text{MoP}}(\cdot; \mathbf{s}; \theta_d, \theta_r, \theta_p)} [Q(\mathbf{s}, \mathbf{a})]. \text{ (Adapter Policy Optimization)} \quad (9)$$

In Eq. (9), the learned policy interacts with the environment rolling out the (s, a, r) tuple. With the frozen distilled knowledge of LLM in π_{distil} , parameterized by $\theta_p^{(1)}$, we fine-tune π_{adapt} , parameterized by $\theta_p^{(2)}$, to adapt the MoP policy Π_{MoP} with LLM prior to the actual RL environment.

3.3.3 Zero Gating Adapter Policy

To eliminate the influence of π_{adapt} on π_{distil} during the offline phase, we adopt the concept of zero gating [29] for initializing the policy. Specifically, the router network’s corresponding expert weights for π_{adapt} are masked with a trainable zero vector. As a result, the MoP token in phase 2 only considers the impact of $\pi_{\text{distil}}(s)$. During phase 3, we enable the training of zero gates, allowing adaptation tokens to progressively inject newly acquired online signals into the MoP policy Π_{MoP} .

4 Experiments

4.1 Experiment Setting

We conduct experiments using the HighwayEnv simulation environment [22]. We involve three driving scenarios with increasing levels of complexity: LANE-3-DENSITY-2, LANE-4-DENSITY-2.5, and LANE-5-DENSITY-3. Detailed task descriptions are delegated to Appendix D. This paper constructs three types of datasets, namely the *random* $\mathcal{D}_{\text{rand}}$, the *LLM-collected* \mathcal{D}_{LLM} , and the *combined* dataset $\mathcal{D}_{\text{off}}^*$. The construction details and optimal ratio for $\mathcal{D}_{\text{off}}^*$ are discussed in Sec. 4.2.

We compare the RAPID performance under the offline phase with several state-of-the-art RL methods, DQN [30], DDQN [31], and CQL [20] respectively. In the online phase, we employ the DQN algorithm as the adaptation method under our RAPID framework. To validate the efficacy of J_{robust} term in Eq. (5), we utilize four various attack methods: Uniform, Gaussian, FGSM, and PGD, to evaluate the robustness of the distilled policy. All baselines are implemented with d3rlpy library [32]. The hyperparameters setting refers to Appendix. E. Each method is trained for a total of 10K training iterations, with evaluations performed per 1K iterations. We employ the same reward function as defined in highway-env-rewards².

²rewards: highway-env.farama.org/rewards

4.2 Fusing LLM Generated Dataset (Phase 1)

To validate the efficacy of the LLM-collected dataset \mathcal{D}_{LLM} , we build the offline dataset by combining it with a random dataset $\mathcal{D}_{\text{rand}}$. We evaluate the cumulative rewards on $\mathcal{D}_{\text{off}} = \text{sample}(\{\mathcal{D}_{\text{LLM}}, \mathcal{D}_{\text{rand}}\}; \{p, 1-p\})$ with two offline algorithms: DDQN [31] and CQL [20], to find the best ratio p . To clarify, $\mathcal{D}_{\text{rand}}$ is sampled using a random behavioural policy, serving as a baseline for data collection. \mathcal{D}_{LLM} is sampled via a pre-trained LLM π_{LLM} . We gather 3K transitions using π_{LLM} for each trail. Therefore, both $\mathcal{D}_{\text{random}}$ and \mathcal{D}_{LLM} dataset contains 15K transitions.

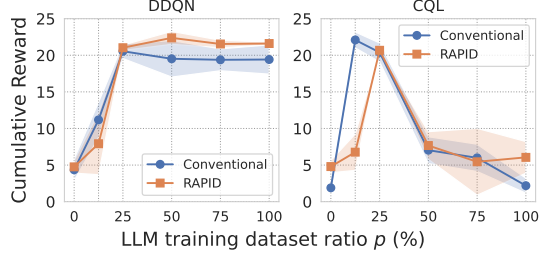


Figure 3: Cumulative reward over different training ratios under offline training framework in HIGHWAY-FAST environment. The result is averaged over 5 random trails.

According to Fig. 3, the pure $\mathcal{D}_{\text{rand}}$ with $p = 0\%$ cannot support a well-trained offline policy. Utilizing only the \mathcal{D}_{LLM} can also harm the performance. However, augmenting offline datasets with partial LLM-generated data can significantly boost policy cumulative reward. With such evidence, we choose $p = 25\%$ in between $12.5\% \sim 50\%$ as a sweet spot and define it as our final $\mathcal{D}_{\text{off}}^*$.

4.3 Offline LLM Knowledge Distillation (Phase 2)

Table 1: The cumulative rewards in **Phase 2**, averaged over 3 seeds. RAPID (with&without J_{robust}) only enable the π_{distil} part (as depicted in Fig. 2) in offline training. RAPID (w/o J_{robust}) distils the LLM knowledge with Eq. (4) while RAPID uses robust distillation Eq. (5). **Blue** / **Orange** indicate the first/second highest return for each buffer. **Bold** denotes the best within each environment.

Environments	Dataset	CQL	DQN	DDQN	RAPID (w/o J_{robust})	RAPID
LANE-3-DENSITY-2	$\mathcal{D}_{\text{rand}}$	3.01 ± 1.49	4.40 ± 1.57	4.86 ± 1.58	3.47 ± 1.45	3.66 ± 1.58
	\mathcal{D}_{LLM}	7.96 ± 1.63	9.14 ± 8.80	10.83 ± 4.94	12.22 ± 7.03	14.18 ± 2.43
	$\mathcal{D}_{\text{off}}^*$	13.06 ± 1.11	8.66 ± 6.93	12.22 ± 7.03	12.72 ± 0.59	15.33 ± 5.30
LANE-4-DENSITY-2.5	$\mathcal{D}_{\text{rand}}$	3.84 ± 2.59	2.41 ± 0.92	1.96 ± 0.52	2.18 ± 0.59	3.60 ± 2.67
	\mathcal{D}_{LLM}	2.56 ± 0.90	3.99 ± 1.18	5.82 ± 6.16	3.27 ± 2.05	4.60 ± 2.69
	$\mathcal{D}_{\text{off}}^*$	7.36 ± 0.60	7.14 ± 6.12	7.61 ± 6.76	10.19 ± 1.30	10.29 ± 0.20
LANE-5-DENSITY-3	$\mathcal{D}_{\text{rand}}$	1.53 ± 0.29	5.59 ± 2.84	3.72 ± 2.85	3.13 ± 0.36	2.16 ± 0.36
	\mathcal{D}_{LLM}	2.23 ± 0.29	5.54 ± 7.98	4.76 ± 1.89	5.26 ± 4.61	1.45 ± 2.11
	$\mathcal{D}_{\text{off}}^*$	5.58 ± 3.93	5.99 ± 4.10	5.05 ± 2.06	5.38 ± 0.63	6.14 ± 2.85

Phase 2 only uses π_{distil} for offline training as described in Sec. 3.3. We evaluate RAPID on three environments, respectively, LANE-3-DENSITY-2, LANE-4-DENSITY-2.5 and LANE-5-DENSITY-3 with three different types of datasets: $\mathcal{D}_{\text{rand}}$, \mathcal{D}_{LLM} and $\mathcal{D}_{\text{off}}^*$ as described in Sec. 4.2. In particular, we collect $\mathcal{D}_{\text{off}}^*$ with LANE-3-DENSITY-2 only, and apply this dataset to trails LANE-3-DENSITY-2- $\mathcal{D}_{\text{off}}^*$, LANE-4-DENSITY-2.5- $\mathcal{D}_{\text{off}}^*$, and LANE-5-DENSITY-3- $\mathcal{D}_{\text{off}}^*$.

We present the offline results in Tab. 1 and observe the following: (1) With \mathcal{D}_{LLM} , policies exhibit better offline performance than $\mathcal{D}_{\text{rand}}$ in general, while $\mathcal{D}_{\text{off}}^*$, as a mixture of above, improve upon both randomly- and LLM-generated datasets. This again confirms our conclusion in Sec. 4.2. (2) Our approach, RAPID, consistently outperforms conventional methods, with RAPID using the mixed $\mathcal{D}_{\text{off}}^*$ achieving the highest rewards overall. (3) J_{robust} does not impact the clean performance under the offline training phase. (4) $\mathcal{D}_{\text{off}}^*$ collected from LANE-3-DENSITY-2 achieves better performance across all tasks, indicating that the LLM-generated dataset contains general knowledge applicable to different tasks with the same state and action spaces.

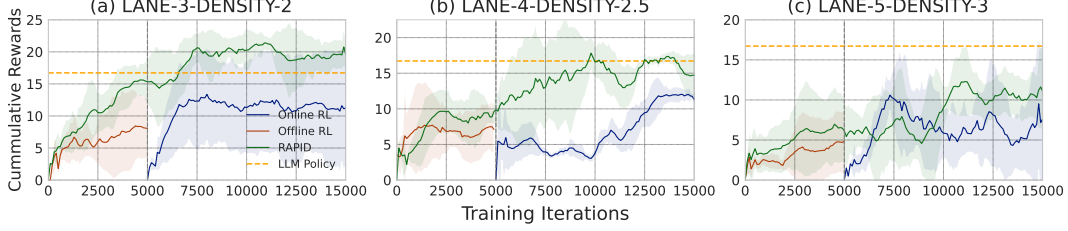


Figure 4: Performance of online adaptation (**Phase 3**) across three environments. Before the 5K-iteration mark, we pre-train the π_{distil} policy of RAPID using the method described in Phase 2. Note that π_{distil} keeps frozen in Phase 3. We report the average performance over 5 random trails.

4.4 Online Adaptation Performance (Phase 3)

To evaluate the online adaptation ability of RAPID, we employ the pre-trained π_{distil} from **Phase 2** (with the collected $\mathcal{D}_{\text{off}}^*$ from LANE-3-DENSITY-2). Then train the π_{adapt} and its zero gate (as depicted in Fig. 2(c)) via interacting with different online environments. We compare it with the vanilla Online RL (DQN) and Offline RL (DQN) without using the RAPID MoP policy. We train the RAPID policy for 5K training epochs during the offline phase, followed by 10K online epochs. The Online DQN starts from the 5K-th epoch.

As depicted in Fig. 4: (1) The cumulative rewards for π_{distil} are sufficiently high, due to the introduced common sense knowledge and reasoning abilities from π_{LLM} . However, the conventional offline RL cannot perform well. (2) With the offline phase pre-trained on LANE-3-DENSITY-2, the online adaptation with RAPID MoP on the same dataset LANE-3-DENSITY-2 (Fig. 4(a)) achieves significantly high rewards. This demonstrates the necessity of online adaptation to generalize knowledge for practical application. (3) We further conduct zero-shot adaptation on offline-unseen dataset LANE-4-DENSITY-2.5 and LANE-5-DENSITY-3. In Fig. 4(b-c), we observe RAPID can achieve competitive performance not only compared to the vanilla online approach, but toward the large π_{LLM} . This highlights the efficacy of the RAPID framework in task adaptation.

4.5 Robust Distillation Performance

We evaluate the robustness of multiple distillation algorithms using 4 different attack methods, respectively, Uniform, Gaussian, FGSM and PGD. Specifically, we employ a 10-step PGD with a designated step size of 0.01. For both FGSM and PGD attacks, the attack radius ϵ is set to 0.1. For Uniform and Gaussian attacks, ϵ is set to 0.2. The observation was normalized before the attack and then denormalized for standard RL policy understanding. In RAPID, we set the β as 0.5 to balance the robustness distillation term according to Eq. (5).

As illustrated in Tab. 2, the conventional methods, Online DQN and Offline DQN, are not able to effectively defend against strong adversarial attacks like FGSM and PGD. Although Offline DQN, which is trained on the dataset $\mathcal{D}_{\text{off}}^*$ partially collected by the LLM policy π_{LLM} . It still struggles to maintain performance under these attacks. RAPID (w/o J_{robust}), which undergoes offline training and online adaptation without using J_{robust} , performs weakly when facing strong adversarial attacks. In contrast, the full RAPID method with J_{robust} demonstrates superior robustness against various adversarial attacks across all three environments. We note that the J_{robust} might approximate the robustness of LLM by building the robust soft label in Eq. 5. Overall, the J_{robust} regularizer plays a crucial role in bolstering the robustness of the model by effectively utilizing the robust knowledge obtained from the LLM-based teacher.

4.6 Ablation Study

MoP Routing Analysis. In Fig. 5, we visualize the contribution of each policy (π_{distil} and π_{adapt}) to the final predicted action at each vehicle position after online adaptation. In general, π_{distil} dom-

Table 2: Adversarial Performance against observation perturbation, averaged over 5 trails. The Offline DQN, RAPID and RAPID (w/o J_{robust}) are trained based on the dataset $\mathcal{D}_{\text{off}}^*$. The RAPID and RAPID (w/o J_{robust}) are processed under offline training and online adaptation, while the Offline DQN only goes through the offline training process. **Bold** indicates the best return against observation perturbation within each environment.

Environments	Method	Clean	Attack Return			
			Uniform	Gaussian	FGSM	PGD
LANE-3-DENSITY-2	Online DQN	12.48 \pm 8.56	11.74 \pm 7.75	10.72 \pm 8.27	2.09 \pm 1.62	1.09 \pm 1.32
	Offline DQN	8.66 \pm 6.93	6.73 \pm 2.04	6.29 \pm 1.28	2.12 \pm 0.23	1.73 \pm 1.04
	RAPID (w/o J_{robust})	19.79 \pm 3.42	17.01 \pm 4.30	15.86 \pm 5.21	3.40 \pm 1.26	1.26 \pm 1.02
	RAPID	20.42 \pm 2.59	20.41 \pm 1.58	20.23 \pm 1.26	15.34 \pm 2.97	14.77 \pm 1.23
LANE-4-DENSITY-2.5	Online DQN	11.58 \pm 0.56	10.49 \pm 4.52	10.18 \pm 4.72	6.03 \pm 0.86	6.12 \pm 0.78
	Offline DQN	7.14 \pm 6.12	5.20 \pm 1.47	6.56 \pm 1.06	2.56 \pm 1.06	2.20 \pm 1.47
	RAPID (w/o J_{robust})	13.79 \pm 3.48	12.87 \pm 1.43	11.61 \pm 5.63	5.53 \pm 3.27	3.26 \pm 1.24
	RAPID	14.34 \pm 2.84	13.63 \pm 5.26	13.91 \pm 7.84	10.87 \pm 2.68	8.39 \pm 2.11
LANE-5-DENSITY-3	Online DQN	6.05 \pm 9.41	6.64 \pm 1.46	5.48 \pm 7.67	1.55 \pm 1.10	1.54 \pm 1.11
	Offline DQN	5.99 \pm 4.10	2.55 \pm 2.10	2.22 \pm 1.99	1.22 \pm 1.03	0.88 \pm 0.58
	RAPID (w/o J_{robust})	8.47 \pm 2.64	4.28 \pm 1.44	3.20 \pm 2.06	0.34 \pm 0.24	0.79 \pm 0.33
	RAPID	7.83 \pm 3.41	5.14 \pm 3.19	5.22 \pm 2.68	2.96 \pm 0.76	1.62 \pm 0.48

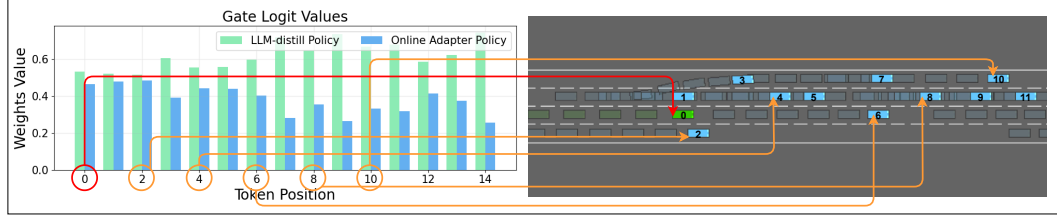


Figure 5: Visualizing the contribution of π_{distil} and π_{adapt} to the final predicted action. The example is randomly sampled via interacting with LANE-4-DENSITY-2.5 using Π_{MoP} . More samples are demonstrated in Appendix B.4.

inates the contribution across all vehicles, as π_{adapt} is initially masked out during offline training. However, after the online phase, π_{adapt} provides a more balanced contribution, especially for the ego vehicle and nearby vehicles (like vehicles 0, 2, 4 in Fig. 5), indicating the effectiveness of online adaptation. Interestingly, π_{distil} still contributes substantially for distant vehicles, suggesting the value of LLM-distilled knowledge in understanding overall traffic context. This demonstrates the efficacy of the MoP approach in integrating knowledge from both the LLM-based teacher and the environment interaction, leveraging the most relevant expertise for each vehicle based on the domain and relative position.

Additional Ablation Studies. Please refer to Appendix B.

5 Conclusion

We propose RAPID, a promising approach for leveraging LLMs’ reasoning abilities and common sense knowledge to enhance the performance of RL agents in heterogeneous autonomous driving tasks. Meanwhile, RAPID overcomes challenges such as the long inference time of LLMs and policy knowledge overwriting. The robust knowledge distillation method enables the student RL policy to inherit the robustness of the LLM teacher.

Limitation and future work. Although we have conducted tests in three distinct autonomous driving environments and validated the closed-loop RL policy in real-time, the scope of the analysis is restricted. The 2D HighwayEnv remains overly simplistic for comprehensive autonomous driving evaluation. To further establish the efficacy of our online adaptation policy, it is necessary to assess its performance with Visual Language Models [33, 34] in more realistic and complex autonomous driving environments, like CARLA [35].

Acknowledgments

If a paper is accepted, the final camera-ready version will (and probably should) include acknowledgments. All acknowledgments go at the end of the paper, including thanks to reviewers who gave useful comments, to colleagues who contributed to the ideas, and to funding agencies and corporate sponsors that provided financial support.

References

- [1] X. Tian, J. Gu, B. Li, Y. Liu, C. Hu, Y. Wang, K. Zhan, P. Jia, X. Lang, and H. Zhao. Drivevlm: The convergence of autonomous driving and large vision-language models. *arXiv preprint arXiv:2402.12289*, 2024.
- [2] Y. Jin, X. Shen, H. Peng, X. Liu, J. Qin, J. Li, J. Xie, P. Gao, G. Zhou, and J. Gong. Surrealdriver: Designing generative driver agent simulation framework in urban contexts based on large language model. *arXiv preprint arXiv:2309.13193*, 2023.
- [3] B. Jin, X. Liu, Y. Zheng, P. Li, H. Zhao, T. Zhang, Y. Zheng, G. Zhou, and J. Liu. Adapt: Action-aware driving caption transformer. In *2023 IEEE International Conference on Robotics and Automation (ICRA)*, pages 7554–7561. IEEE, 2023.
- [4] D. Fu, X. Li, L. Wen, M. Dou, P. Cai, B. Shi, and Y. Qiao. Drive like a human: Rethinking autonomous driving with large language models. *arXiv preprint arXiv:2307.07162*, 2023.
- [5] L. Wen, D. Fu, X. Li, X. Cai, T. Ma, P. Cai, M. Dou, B. Shi, L. He, and Y. Qiao. Dilu: A knowledge-driven approach to autonomous driving with large language models. *arXiv preprint arXiv:2309.16292*, 2023.
- [6] L. Chen, O. Sinavski, J. Hünemann, A. Karnsund, A. J. Willmott, D. Birch, D. Maund, and J. Shotton. Driving with llms: Fusing object-level vector modality for explainable autonomous driving. *arXiv preprint arXiv:2310.01957*, 2023.
- [7] T. Carta, C. Romac, T. Wolf, S. Lamprier, O. Sigaud, and P.-Y. Oudeyer. Grounding large language models in interactive environments with online reinforcement learning. In *International Conference on Machine Learning*, pages 3676–3713. PMLR, 2023.
- [8] B. Huang, M. Chen, Y. Wang, J. Lu, M. Cheng, and W. Wang. Boosting accuracy and robustness of student models via adaptive adversarial distillation. In *Proceedings of the IEEE/CVF Conference on Computer Vision and Pattern Recognition (CVPR)*, pages 24668–24677, June 2023.
- [9] B. Zi, S. Zhao, X. Ma, and Y.-G. Jiang. Revisiting adversarial robustness distillation: Robust soft labels make student better. In *Proceedings of the IEEE/CVF International Conference on Computer Vision*, pages 16443–16452, 2021.
- [10] M. Goldblum, L. Fowl, S. Feizi, and T. Goldstein. Adversarially robust distillation. In *Proceedings of the AAAI conference on artificial intelligence*, volume 34, pages 3996–4003, 2020.
- [11] J. Zhu, J. Yao, B. Han, J. Zhang, T. Liu, G. Niu, J. Zhou, J. Xu, and H. Yang. Reliable adversarial distillation with unreliable teachers. *arXiv preprint arXiv:2106.04928*, 2021.
- [12] R. Shi, Y. Liu, Y. Ze, S. S. Du, and H. Xu. Unleashing the power of pre-trained language models for offline reinforcement learning. *arXiv preprint arXiv:2310.20587*, 2023.
- [13] Z. Zhou, B. Hu, P. Zhang, C. Zhao, and B. Liu. Large language model is a good policy teacher for training reinforcement learning agents. *arXiv preprint arXiv:2311.13373*, 2023.
- [14] W. Huang, P. Abbeel, D. Pathak, and I. Mordatch. Language models as zero-shot planners: Extracting actionable knowledge for embodied agents, 2022.

- [15] J. Wei, M. Bosma, V. Y. Zhao, K. Guu, A. W. Yu, B. Lester, N. Du, A. M. Dai, and Q. V. Le. Finetuned language models are zero-shot learners, 2022.
- [16] T. Brown, B. Mann, N. Ryder, M. Subbiah, J. D. Kaplan, P. Dhariwal, A. Neelakantan, P. Shyam, G. Sastry, A. Askell, et al. Language models are few-shot learners. *Advances in neural information processing systems*, 33:1877–1901, 2020.
- [17] Z. Wang, X. Pan, D. Yu, D. Yu, J. Chen, and H. Ji. Zemi: Learning zero-shot semi-parametric language models from multiple tasks. *arXiv preprint arXiv:2210.00185*, 2022.
- [18] Y. Gu, P. Ke, X. Zhu, and M. Huang. Learning instructions with unlabeled data for zero-shot cross-task generalization. *arXiv preprint arXiv:2210.09175*, 2022.
- [19] A. Kumar, J. Fu, M. Soh, G. Tucker, and S. Levine. Stabilizing off-policy q-learning via bootstrapping error reduction. *Advances in Neural Information Processing Systems*, 32, 2019.
- [20] A. Kumar, A. Zhou, G. Tucker, and S. Levine. Conservative q-learning for offline reinforcement learning, 2020.
- [21] K. Schweighofer, M.-c. Dinu, A. Radler, M. Hofmarcher, V. P. Patil, A. Bitto-Nemling, H. Eghbal-zadeh, and S. Hochreiter. A dataset perspective on offline reinforcement learning. In *Conference on Lifelong Learning Agents*, pages 470–517. PMLR, 2022.
- [22] E. Leurent. An environment for autonomous driving decision-making. <https://github.com/eleurent/highway-env>, 2018.
- [23] OpenAI. Introducing chatgpt. <https://openai.com/index/chatgpt/>, 2023.
- [24] S. Yao, J. Zhao, D. Yu, N. Du, I. Shafran, K. Narasimhan, and Y. Cao. React: Synergizing reasoning and acting in language models. *arXiv preprint arXiv:2210.03629*, 2022.
- [25] R. Yang, C. Bai, X. Ma, Z. Wang, C. Zhang, and L. Han. Rorl: Robust offline reinforcement learning via conservative smoothing. *Advances in Neural Information Processing Systems*, 35: 23851–23866, 2022.
- [26] A. Clark, D. de Las Casas, A. Guy, A. Mensch, M. Paganini, J. Hoffmann, B. Damoc, B. Hechtman, T. Cai, S. Borgeaud, et al. Unified scaling laws for routed language models. In *International conference on machine learning*, pages 4057–4086. PMLR, 2022.
- [27] H. Hazimeh, Z. Zhao, A. Chowdhery, M. Sathiamoorthy, Y. Chen, R. Mazumder, L. Hong, and E. Chi. Dselect-k: Differentiable selection in the mixture of experts with applications to multi-task learning. *Advances in Neural Information Processing Systems*, 34:29335–29347, 2021.
- [28] Y. Zhou, T. Lei, H. Liu, N. Du, Y. Huang, V. Zhao, A. M. Dai, Q. V. Le, J. Laudon, et al. Mixture-of-experts with expert choice routing. *Advances in Neural Information Processing Systems*, 35:7103–7114, 2022.
- [29] R. Zhang, J. Han, C. Liu, P. Gao, A. Zhou, X. Hu, S. Yan, P. Lu, H. Li, and Y. Qiao. Llama-adapter: Efficient fine-tuning of language models with zero-init attention, 2023.
- [30] V. Mnih, K. Kavukcuoglu, D. Silver, A. A. Rusu, J. Veness, M. G. Bellemare, A. Graves, M. Riedmiller, A. K. Fidjeland, G. Ostrovski, et al. Human-level control through deep reinforcement learning. *nature*, 518(7540):529–533, 2015.
- [31] H. Van Hasselt, A. Guez, and D. Silver. Deep reinforcement learning with double q-learning. In *Proceedings of the AAAI conference on artificial intelligence*, volume 30, 2016.
- [32] T. Seno and M. Imai. d3rlpy: An offline deep reinforcement learning library. *The Journal of Machine Learning Research*, 23(1):14205–14224, 2022.

- [33] C. Sima, K. Renz, K. Chitta, L. Chen, H. Zhang, C. Xie, P. Luo, A. Geiger, and H. Li. Drivelm: Driving with graph visual question answering. *arXiv preprint arXiv:2312.14150*, 2023.
- [34] W. Wang, J. Xie, C. Hu, H. Zou, J. Fan, W. Tong, Y. Wen, S. Wu, H. Deng, Z. Li, et al. Drivelm: Aligning multi-modal large language models with behavioral planning states for autonomous driving. *arXiv preprint arXiv:2312.09245*, 2023.
- [35] A. Dosovitskiy, G. Ros, F. Codevilla, A. Lopez, and V. Koltun. Carla: An open urban driving simulator. In *Conference on robot learning*, pages 1–16. PMLR, 2017.
- [36] S. Levine, A. Kumar, G. Tucker, and J. Fu. Offline reinforcement learning: Tutorial, review, and perspectives on open problems, 2020.
- [37] V. Mnih, K. Kavukcuoglu, D. Silver, A. Graves, I. Antonoglou, D. Wierstra, and M. Riedmiller. Playing atari with deep reinforcement learning. *arXiv preprint arXiv:1312.5602*, 2013.
- [38] X. Yin, S. Wu, J. Liu, M. Fang, X. Zhao, X. Huang, and W. Ruan. Rerogrl: Representation-based robustness in goal-conditioned reinforcement learning, 2023.
- [39] S. Fujimoto, D. Meger, and D. Precup. Off-policy deep reinforcement learning without exploration, 2019.
- [40] I. Kostrikov, A. Nair, and S. Levine. Offline reinforcement learning with implicit q-learning. In *International Conference on Learning Representations*, 2022. URL <https://openreview.net/forum?id=68n2s9ZJWF8>.
- [41] S. Fujimoto and S. S. Gu. A minimalist approach to offline reinforcement learning, 2021.
- [42] Y. Wu, S. Zhai, N. Srivastava, J. M. Susskind, J. Zhang, R. Salakhutdinov, and H. Goh. Uncertainty weighted offline reinforcement learning, 2021. URL <https://openreview.net/forum?id=7hMenh--8g>.
- [43] Y. Gu, L. Dong, F. Wei, and M. Huang. Knowledge distillation of large language models, 2023.
- [44] C.-Y. Hsieh, C.-L. Li, C.-K. Yeh, H. Nakhost, Y. Fujii, A. Ratner, R. Krishna, C.-Y. Lee, and T. Pfister. Distilling step-by-step! outperforming larger language models with less training data and smaller model sizes. *arXiv preprint arXiv:2305.02301*, 2023.
- [45] OpenAI. Gpt4 report. <https://arxiv.org/abs/2303.08774>, 2023.
- [46] H. Touvron, L. Martin, K. Stone, P. Albert, A. Almahairi, Y. Babaei, N. Bashlykov, S. Batra, P. Bhargava, S. Bhosale, et al. Llama 2: Open foundation and fine-tuned chat models. *arXiv preprint arXiv:2307.09288*, 2023.
- [47] A. Zhou, K. Yan, M. Shlapentokh-Rothman, H. Wang, and Y.-X. Wang. Language agent tree search unifies reasoning acting and planning in language models. *arXiv preprint arXiv:2310.04406*, 2023.
- [48] B. Y. Lin, Y. Fu, K. Yang, P. Ammanabrolu, F. Brahman, S. Huang, C. Bhagavatula, Y. Choi, and X. Ren. Swiftsage: A generative agent with fast and slow thinking for complex interactive tasks. *arXiv preprint arXiv:2305.17390*, 2023.
- [49] X. Deng, Y. Gu, B. Zheng, S. Chen, S. Stevens, B. Wang, H. Sun, and Y. Su. Mind2web: Towards a generalist agent for the web. *arXiv preprint arXiv:2306.06070*, 2023.
- [50] S. Zhou, F. F. Xu, H. Zhu, X. Zhou, R. Lo, A. Sridhar, X. Cheng, Y. Bisk, D. Fried, U. Alon, et al. Webarena: A realistic web environment for building autonomous agents. *arXiv preprint arXiv:2307.13854*, 2023.

- [51] K. Nottingham, P. Ammanabrolu, A. Suhr, Y. Choi, H. Hajishirzi, S. Singh, and R. Fox. Do embodied agents dream of pixelated sheep?: Embodied decision making using language guided world modelling. *arXiv preprint arXiv:2301.12050*, 2023.
- [52] C. H. Song, J. Wu, C. Washington, B. M. Sadler, W.-L. Chao, and Y. Su. Llm-planner: Few-shot grounded planning for embodied agents with large language models. In *Proceedings of the IEEE/CVF International Conference on Computer Vision*, pages 2998–3009, 2023.
- [53] Z. Wang, S. Cai, A. Liu, X. Ma, and Y. Liang. Describe, explain, plan and select: Interactive planning with large language models enables open-world multi-task agents. *arXiv preprint arXiv:2302.01560*, 2023.
- [54] Wayve. Lingo-1: Exploring natural language for autonomous driving. <https://wayve.ai/thinking/lingo-natural-language-autonomous-driving/>, 2023.
- [55] Z. Yang, X. Jia, H. Li, and J. Yan. A survey of large language models for autonomous driving. *arXiv preprint arXiv:2311.01043*, 2023.
- [56] Y. Fu, H. Peng, L. Ou, A. Sabharwal, and T. Khot. Specializing smaller language models towards multi-step reasoning. In A. Krause, E. Brunskill, K. Cho, B. Engelhardt, S. Sabato, and J. Scarlett, editors, *Proceedings of the 40th International Conference on Machine Learning*, volume 202 of *Proceedings of Machine Learning Research*, pages 10421–10430. PMLR, 23–29 Jul 2023. URL <https://proceedings.mlr.press/v202/fu23d.html>.
- [57] L. Beyer, X. Zhai, A. Royer, L. Markeeva, R. Anil, and A. Kolesnikov. Knowledge distillation: A good teacher is patient and consistent. In *Proceedings of the IEEE/CVF conference on computer vision and pattern recognition*, pages 10925–10934, 2022.
- [58] P. West, C. Bhagavatula, J. Hessel, J. Hwang, L. Jiang, R. Le Bras, X. Lu, S. Welleck, and Y. Choi. Symbolic knowledge distillation: from general language models to common-sense models. In M. Carpuat, M.-C. de Marneffe, and I. V. Meza Ruiz, editors, *Proceedings of the 2022 Conference of the North American Chapter of the Association for Computational Linguistics: Human Language Technologies*, pages 4602–4625, Seattle, United States, July 2022. Association for Computational Linguistics. doi:10.18653/v1/2022.naacl-main.341. URL <https://aclanthology.org/2022.naacl-main.341>.
- [59] F. Iliopoulos, V. Kontonis, C. Baykal, G. Menghani, K. Trinh, and E. Vee. Weighted distillation with unlabeled examples. In A. H. Oh, A. Agarwal, D. Belgrave, and K. Cho, editors, *Advances in Neural Information Processing Systems*, 2022. URL <https://openreview.net/forum?id=M34VHvEU4NZ>.
- [60] R. Smith, J. A. Fries, B. Hancock, and S. H. Bach. Language models in the loop: Incorporating prompting into weak supervision. *arXiv preprint arXiv:2205.02318*, 2022.
- [61] S. Wang, Y. Liu, Y. Xu, C. Zhu, and M. Zeng. Want to reduce labeling cost? GPT-3 can help. In M.-F. Moens, X. Huang, L. Specia, and S. W.-t. Yih, editors, *Findings of the Association for Computational Linguistics: EMNLP 2021*, pages 4195–4205, Punta Cana, Dominican Republic, Nov. 2021. Association for Computational Linguistics. doi:10.18653/v1/2021.findings-emnlp.354. URL <https://aclanthology.org/2021.findings-emnlp.354>.
- [62] A. Vaswani, N. Shazeer, N. Parmar, J. Uszkoreit, L. Jones, A. N. Gomez, Ł. Kaiser, and I. Polosukhin. Attention is all you need. *Advances in neural information processing systems*, 30, 2017.

A Related Work

A.1 Offline RL for Autonomous Driving

Offline RL algorithms are designed to learn policies from a static dataset, eliminating the need for interaction with the real environment [36]. Compared to conventional online RL [37] and the extended goal-conditioned RL [38], this approach is especially beneficial in scenarios where such interaction is prohibitively expensive or risky, such as in autonomous driving. Offline RL algorithms have demonstrated the capability to surpass expert-level performance [39, 20, 40]. In general, these algorithms employ policy regularization [39, 41] and out-of-distribution (OOD) penalization [20, 42] as strategies to prevent value overestimation. In this paper, we pioneer utilising the LLM-generated data to train the offline RL. Although there have been several works [43, 44] focus on distillation for LLM, none of them considers distilling to RL.

A.2 LLM for Autonomous Driving

Recent advancements in LLMs [16, 45, 46] demonstrate their powerful embodied abilities, providing the possibility to distil knowledge from humans to autonomous systems. LLMs exhibit a strong aptitude for general reasoning [47, 48], web agents [49, 50], and embodied robotics [51, 52, 53]. Inspired by the superior capability of common sense of LLM-based agents, a substantial body of research is dedicated to LLM-based autonomous driving. Wayve [54] introduced an open-loop driving commentator called LINGO-1, which integrates vision, language, and action to enhance the interpretation and training of driving models. DiLu [5] developed a framework utilizing LLMs as agents for closed-loop driving tasks, with a memory module to record experiences. To enhance the stability and generalization performance, [4] utilised reasoning, interpretation, and memorization of LLM to enhance autonomous driving. More research works for this vibrant field were summarised in [55]. However, all these methods require huge resources, long inference time, and unstable performance. To bridge this gap, we propose a knowledge distillation framework, from LLM to RL, which enhances the applicability and stability of real-world autonomous driving.

A.3 Distillation for LLM

Knowledge distillation has proven successful in transferring knowledge from large-scale, more competent teacher models to small-scale student models, making them more affordable for practical applications [56, 57, 58]. This method facilitates learning from limited labelled data, as the larger teacher model is commonly employed to generate a training dataset with noisy pseudo-labels [59, 60, 61]. Further, [44] involves extracting rationales from LLMs as additional supervisory signals to train small-scale models within a multi-task framework. [43] utilises reverse Kullback-Leibler divergence to ensure that the student model does not overestimate the low-probability regions in the teacher distribution. Currently, knowledge distillation from LLM to RL for autonomous driving remains unexplored.

B Additional Experiments

B.1 Comparison between MLP and RAPID(Attentive) based Policy

Table 3: Comparison between MLP and RAPID(Attentive) based policy under offline RL training. **Bold** denotes the best among each environment. Results are averaged across 3 seeds.

Environments	Dataset	MLP Policy			RAPID(Attentive) Policy		
		CQL	DQN	DDQN	CQL	DQN	DDQN
LANE-3-DENSITY-2	$\mathcal{D}_{\text{rand}}$	3.01 ± 1.49	4.40 ± 1.57	4.86 ± 1.58	3.50 ± 0.84	3.66 ± 1.58	2.56 ± 0.18
	\mathcal{D}_{LLM}	7.96 ± 1.63	9.14 ± 8.80	10.83 ± 4.94	12.81 ± 7.51	14.18 ± 2.43	5.65 ± 3.13
	$\mathcal{D}_{\text{off}}^*$	13.06 ± 1.11	8.66 ± 6.93	12.22 ± 7.03	12.84 ± 0.68	15.33 ± 5.30	13.95 ± 1.27
LANE-4-DENSITY-2.5	$\mathcal{D}_{\text{rand}}$	3.84 ± 2.59	2.41 ± 0.92	1.96 ± 0.52	6.69 ± 3.82	3.60 ± 2.67	1.70 ± 0.46
	\mathcal{D}_{LLM}	2.56 ± 0.90	3.99 ± 1.18	5.82 ± 6.16	5.98 ± 1.30	4.60 ± 2.69	2.23 ± 0.72
	$\mathcal{D}_{\text{off}}^*$	7.36 ± 0.60	7.14 ± 6.12	7.61 ± 6.76	8.14 ± 0.87	10.29 ± 0.20	3.16 ± 0.31
LANE-5-DENSITY-3	$\mathcal{D}_{\text{rand}}$	1.53 ± 0.29	5.59 ± 2.84	3.72 ± 2.85	2.58 ± 1.09	2.16 ± 0.36	1.83 ± 1.48
	\mathcal{D}_{LLM}	2.23 ± 0.29	5.54 ± 7.98	4.76 ± 1.89	2.28 ± 1.65	1.45 ± 2.11	2.33 ± 0.66
	$\mathcal{D}_{\text{off}}^*$	5.58 ± 3.93	5.99 ± 4.10	5.05 ± 2.06	3.37 ± 1.61	6.14 ± 2.85	3.17 ± 0.41

To verify the contribution of the RAPID(Attentive) architecture (as shown in Fig. 8) in the offline training phase, we conduct extra experiments in this section. As illustrated in Tab. 3, we compared the DQN, DDQN, and CQL under MLP and RAPID architecture, respectively. As the environment complexity increases, the performance gap between RAPID and MLP narrows, suggesting RAPID handles simpler environments more effectively. In summary, we conclude: (1) the RAPID + DQN method achieves the best performance among all methods, thus we choose DQN as the backbone of RAPID for offline training. (2) The attentive architecture demonstrates superior performance compared to MLP, particularly in less complex environments.

B.2 Impact of J_{robust}

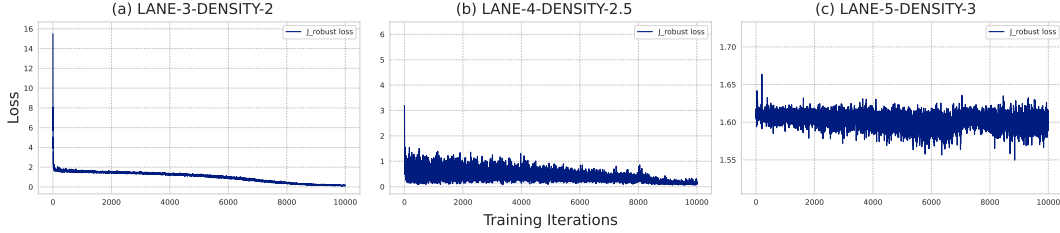


Figure 6: Offline training J_{robust} loss term under the LANE-3-DENSITY-2- $\mathcal{D}_{\text{off}}^*$.

Building upon the results presented in Fig. 6, we provide an analysis of the impact of J_{robust} among three environments. The experiment setup is the same as Sec. 4.3. The RAPID is trained 10K epochs based on LANE-3-DENSITY-2- $\mathcal{D}_{\text{off}}^*$, LANE-4-DENSITY-2.5- $\mathcal{D}_{\text{off}}^*$, and LANE-5-DENSITY-3- $\mathcal{D}_{\text{off}}^*$. From Fig. 6, we observe that the J_{robust} gradually decreased and converged to 0 during the training process. The experimental results align with our results in Tab. 2, as the defense mechanism demonstrates superior performance in both LANE-3-DENSITY-2 and LANE-4-DENSITY-2.5. In the more complex LANE-5-DENSITY-3 environment, the loss remains relatively high, around 1.6, which leads to suboptimal defense performance compared to the other scenarios. This suggests that the increased complexity and vehicle density in this setting pose additional challenges for the defense mechanism. Overall, the consistency across different settings highlights the robustness and effectiveness of our approach.

B.3 Impact of β

Table 4: Adversarial Performance of different β parameters against observation perturbation.

Environments	Method	Clean	Uniform	Attack Return		
				Gaussian	FGSM	PGD
LANE-3-DENSITY-2	RAPID (w/o J_{robust})	19.79 \pm 3.42	17.01 \pm 4.30	15.86 \pm 5.21	3.40 \pm 1.26	1.26 \pm 1.02
	RAPID ($\beta = 0.1$)	20.74 \pm 3.66	21.22 \pm 2.95	20.75 \pm 3.43	10.97 \pm 3.23	10.24 \pm 2.67
	RAPID ($\beta = 0.5$)	20.42 \pm 2.59	20.41 \pm 1.58	20.23 \pm 1.26	15.34 \pm 2.97	14.77 \pm 1.23
	RAPID ($\beta = 0.8$)	18.36 \pm 3.46	18.23 \pm 3.98	17.68 \pm 2.54	13.51 \pm 4.14	11.68 \pm 4.11
LANE-4-DENSITY-2.5	RAPID (w/o J_{robust})	13.79 \pm 3.48	12.87 \pm 1.43	11.61 \pm 5.63	5.53 \pm 3.27	3.26 \pm 1.24
	RAPID ($\beta = 0.1$)	14.12 \pm 1.76	12.66 \pm 4.87	11.38 \pm 6.29	8.17 \pm 3.75	7.13 \pm 2.42
	RAPID ($\beta = 0.5$)	14.34 \pm 2.84	13.63 \pm 5.26	13.91 \pm 7.84	10.87 \pm 2.68	8.39 \pm 2.11
	RAPID ($\beta = 0.8$)	14.21 \pm 5.23	12.24 \pm 3.97	12.68 \pm 4.25	8.69 \pm 3.24	9.16 \pm 4.13
LANE-5-DENSITY-3	RAPID (w/o J_{robust})	8.47 \pm 2.64	4.28 \pm 1.44	3.20 \pm 2.06	0.34 \pm 0.24	0.79 \pm 0.33
	RAPID ($\beta = 0.1$)	6.98 \pm 4.84	6.29 \pm 4.59	6.21 \pm 2.96	1.90 \pm 1.67	2.19 \pm 1.23
	RAPID ($\beta = 0.5$)	7.83 \pm 3.41	5.14 \pm 3.19	5.22 \pm 2.68	2.96 \pm 0.76	1.62 \pm 0.48
	RAPID ($\beta = 0.8$)	6.17 \pm 2.19	4.13 \pm 4.28	5.77 \pm 3.56	2.89 \pm 0.32	2.67 \pm 0.89

To investigate the effect of various β values (hyperparameter in Eq. 5), we compare $\beta \in \{0.1, 0.5, 0.8\}$ on LANE-3-DENSITY-2, LANE-4-DENSITY-2.5, and LANE-5-DENSITY-3, respectively. The results are illustrated in Tab. 4. Based on the results presented in Tab. 4, we make several observations regarding the impact of the β on the performance of our robust distillation approach. When setting $\beta = 0.8$, we notice a decline in the clean performance across all three environments. This degradation can be attributed to the increased emphasis on adversarial examples during the training process, which may lead to a trade-off with clean accuracy. On the other hand, when setting $\beta = 0.1$, the attack return is relatively lower compared to other settings. This suggests that the adversarial training strength may not be sufficient to provide adequate robustness against adversarial perturbations. Considering these findings, we determine that setting $\beta = 0.5$ strikes a balance between maintaining clean performance and achieving satisfactory robustness.

B.4 Visualization the of π_{distil} and π_{adapt}

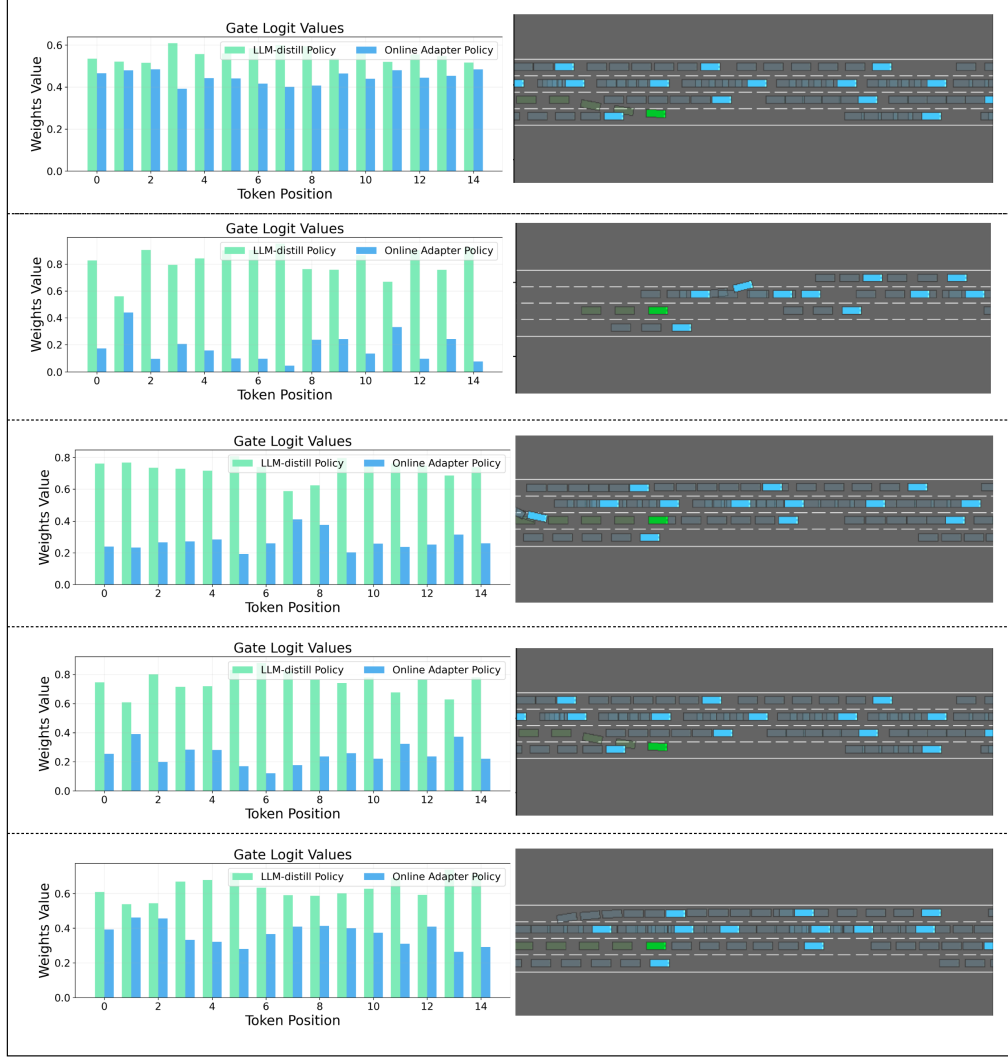


Figure 7: Five more random examples on visualizing the contribution of π_{distil} and π_{adapt} (from the router) to the final predicted action in LANE-4-DENSITY-2.5 using Π_{MoP} .

C Network Implementation

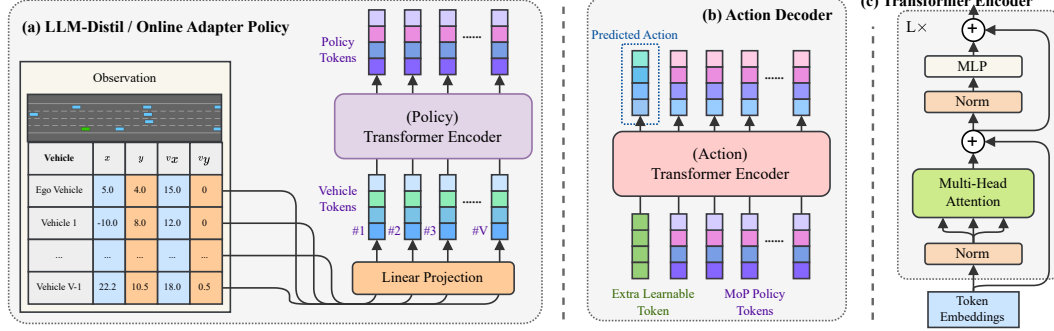


Figure 8: Architecture of (a) Policy networks (transformer encoders) $\pi_{\text{distil}}(\cdot)$ and $\pi_{\text{adapt}}(\cdot)$; (b) Action decoder (transformer encoder) $\text{dec}(\cdot)$; (c) The transformer backbone (encoder-only).

C.1 Transformer Encoder

We employ the same encoder-only transformer f_{TransE} as [62].

C.2 Policy Networks

The policy network consist of a linear projection and a transformer encoder that take the projected state as input. Let state $\mathbf{s} \in \mathbb{R}^{V \times F}$. The policy network first project $\mathbf{s} \rightarrow \mathbf{s}_v \in \mathbb{R}^{V \times F'}$ with a trainable linear projection, then regard \mathbf{s}_v as the input token for the transformer. The transformer then processes these embeddings through $[0, L]$ layers of self-attention and feedforward networks, in our case, we set $L = 2$. Mathematically, for each layer $l \in [0, L]$, the $\pi_{\text{distil}}/\pi_{\text{adapt}}$ computes the following: $\mathbf{s}_p \leftarrow f_{\text{TransE}}^{\text{policy}}(f_{\text{Proj}}(\mathbf{s})) \in \mathbb{R}^{V \times D}$.

C.3 Action Decoder

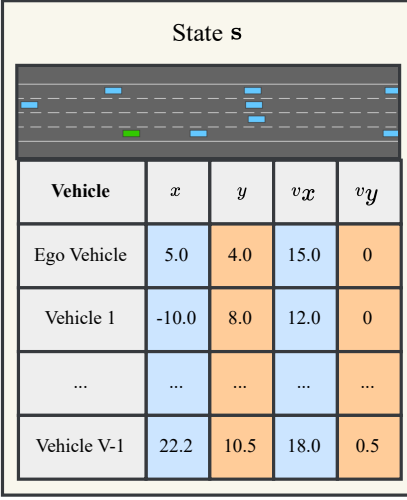
The action decoder transforms encoded state representations into an action using another transformer encoder. It takes the mix-of-policy token from the routed policy networks as input. Given the routed MoP token $\mathbf{s}_m \in \mathbb{R}^{V \times D}$, we first concatenate \mathbf{s}_m with an extra learnable token $\mathbf{s}_e \in \mathbb{R}^{1 \times D}$, then put $\text{concat}(\mathbf{s}_m \parallel \mathbf{s}_e) \in \mathbb{R}^{(V+1) \times D}$ into the transformer encoder. We regard the first output token as the action token. Essentially, $\text{dec} : \mathbb{R}^{V \times D} \rightarrow \mathbb{R}^A$ computes: $\mathbf{a} \leftarrow f_{\text{TransE}}^{\text{action}}(\text{concat}(\mathbf{s}_m \parallel \mathbf{s}_e))_{0,:} \in \mathbb{R}^{1 \times A}$.

D Environment Details

Each of these three environments has continuous state and discrete action space. The maximum episode horizon is defined as 30. Tab. 5 describes the configuration for the highway environment in a reinforcement learning setting. The observation configuration defines the type of observation utilized, which is specified as KinematicsObservation. This observation type represents the surrounding vehicles as a $V \times F$ array, where V denotes the number of nearby vehicles and F represents the size of the feature set describing each vehicle. The specific features included in the observation are listed in the features field of the configuration. The KinematicsObservation provides essential information about the neighbouring vehicles, such as their presence, positions in the x-y coordinate system, and velocities along the x and y axes. These features are represented as absolute values, independent of the agent's frame of reference, and are not subjected to any normalization process. Fig. 9 demonstrates the state features under KinematicObservation setting, in which we introduce the vehicle feature tokenization in Sec. 3.3.

Table 5: Highway Environment Configuration

Parameter	Value
Observation Type	KinematicsObservation
Observation Features	presence, x , y , v_x , v_y
Observation Absolute	True
Observation Normalize	False
Observation Vehicles Count	15
Observation See Behind	True
Action Type	DiscreteMetaAction
Action Target Speeds	np.linspace(0, 32, 9)
Lanes Count	3, (4, 5)
Duration	30
Vehicles Density	2, (2.5, 3)
Show Trajectories	True
Render Agent	True



State s				
Vehicle	x	y	v_x	v_y
Ego Vehicle	5.0	4.0	15.0	0
Vehicle 1	-10.0	8.0	12.0	0
...
Vehicle V-1	22.2	10.5	18.0	0.5

Figure 9: State features under KinematicObservation setting.

E Hyperparameters

In this work, conventional DQN, DDQN and CQL share the same MLP network architectures. For all experiments, the hyperparameters of our backbone architectures and algorithms are reported in Tab. 6. Our implementation is based on d3rlpy [32], which is open-sourced.

Table 6: Hyperparameters for conventional Offline RL methods.

	Hyperparameter	Value		Hyperparameter	Value		Hyperparameter	Value
DQN	Batch size	32	DDQN	Batch size	32	CQL	Batch size	64
	Learning rate	5×10^{-3}		Learning rate	5×10^{-4}		Learning rate	5×10^{-4}
	Target network update interval	50		Target network update interval	50		Target network update interval	50
	Total timesteps	10000		Total timesteps	10000		Total timesteps	10000
	Timestep per epoch	100		Timestep per epoch	100		Timestep per epoch	100
	Buffer capacity	1×10^5		Buffer capacity	1×10^5		Buffer capacity	1×10^5
	Number of Tests	10		Number of Tests	10		Number of Tests	10
	Critic hidden dim	256		Critic hidden dim	256		Critic hidden dim	256
	Critic hidden layers	2		Critic hidden layers	2		Critic hidden layers	2
	Critic activation function	ReLU		Critic activation function	ReLU		Critic activation function	ReLU

F Prompt Setup

In this section, we detail the specific prompt design and give an example of the interaction between the LLM-based agent and the environment.

Prefix Prompt. As shown in Fig. 10, the Prefix Prompt part primarily consists of an introduction to the autonomous driving task, a description of the scenario, common sense rules, and instructions for the output format. The previous decision and explanation are obtained from the experience buffer. The current scenario information plays an important role while making decision, and it is dynamically generated based on the current decision frame. The driving scenario description contains information about the ego and surrounding vehicles' speed and positions. The common sense rules section embeds the driving style to guide the vehicle's behaviour. Finally, the final answer format is constructed to output the discrete actions and construct the closed-loop simulation on HighwayEnv.

Interaction. We demonstrate one example to make readers better understand the reasoning process of GPT-3.5. As shown in Fig. 11, the ego car initially checks the available actions and related safety outcomes. On the first round of thought, GPT-3.5 tries to understand the situation of the ego car and checks the available lanes for decision-making. After several rounds of interaction, it checks whether the action `keep speed` is safe with vehicle 7. Finally, it outputs the decision `idle` and explains that maintaining the current speed and lane can keep a safe distance from surrounding cars.

Prefix Prompt

You, the 'ego' car, are now driving a car on a highway. You have already drive for 6 seconds.

The decision you made LAST time step was *keepspeed*. Your explanation was 'Maintaining the current speed and lane is chosen to ensure safety by keeping a safe distance from the vehicle ahead and adhering to the rules against frequent lane changes. This decision promotes safe and predictable driving behavior.'

Here is the current scenario:

```
json
{
  "lanes": [
    {
      "id": "lane_0",
      "lane index": 0,
      "left_lanes": [],
      "right_lanes": ["lane_1", "lane_2", "lane_3"],
      "id": "lane_1",
      "lane index": 1,
      "left_lanes": ["lane_0"],
      "right_lanes": ["lane_2", "lane_3"],
      "id": "lane_2",
      "lane index": 2,
      "left_lanes": ["lane_0", "lane_1"],
      "right_lanes": ["lane_3"],
      "id": "lane_3",
      "lane index": 3,
      "left_lanes": ["lane_0", "lane_1", "lane_2"],
      "right_lanes": []
    ]
  ],
  "vehicles": [
    {
      "id": "ego",
      "current lane": "lane_1",
      "lane position": 302.19,
      "speed": 16.12,
      "id": "veh1",
      "current lane": "lane_2",
      "lane position": 309.72,
      "speed": 5.08,
      "id": "veh2",
      "current lane": "lane_3",
      "lane position": 292.77,
      "speed": 10.45,
      "id": "veh3",
      "current lane": "lane_0",
      "lane position": 318.89,
      "speed": 16.87,
      "id": "veh4",
      "current lane": "lane_3",
      "lane position": 324.43,
      "speed": 18.29,
      "id": "veh5",
      "current lane": "lane_0",
      "lane position": 279.48,
      "speed": 14.07,
      "id": "veh6",
      "current lane": "lane_2",
      "lane position": 333.48,
      "speed": 10.26,
      "id": "veh7",
      "current lane": "lane_1",
      "lane position": 343.87,
      "speed": 17.89,
      "id": "veh8",
      "current lane": "lane_0",
      "lane position": 358.62,
      "speed": 19.13,
      "id": "veh9",
      "current lane": "lane_2",
      "lane position": 362.78,
      "speed": 14.48,
      "id": "veh10",
      "current lane": "lane_3",
      "lane position": 370.8,
      "speed": 18.66,
      "id": "veh11",
      "current lane": "lane_2",
      "lane position": 399.43,
      "speed": 18.26,
      "id": "veh12",
      "current lane": "lane_1",
      "lane position": 399.86,
      "speed": 15.43,
      "id": "veh13",
      "current lane": "lane_3",
      "lane position": 422.64,
      "speed": 16.65,
      "id": "veh14",
      "current lane": "lane_0",
      "lane position": 429.1,
      "speed": 17.0
    }
  ],
  "ego_info": {
    "id": "ego",
    "current lane": "lane_1",
    "lane position": 302.19,
    "speed": 16.12
  }
}
```

Please make decision for the ego car. You have to describe the state of the *ego*, then analyze the possible actions, and finally output your decision.

There are several rules you need to follow when you drive on a highway:

1. Try to keep a safe distance to the car in front of you.
2. If there is no safe decision, just slowing down.
3. DONOT change lane frequently. If you want to change lane, double-check the safety of vehicles on target lane.

Let's think step by step. Once you made a final decision, output it in the following format:

Final Answer:

```
"decision": {"ego car's decision, ONE of the available actions"},
"explanations": {"your explanation about your decision, described your suggestions to the driver"}
```

Figure 10: Prefix Prompt before interacting with HighwayEnv.

Interaction

Observation:

You can ONLY use one of the following actions:

IDLE--remain in the current lane with current speed;

LANE_LEFT--change lane to the left of the current lane,;

LANE_RIGHT--change lane to the right of the current lane;

FASTER--accelerate the vehicle;

SLOWER--decelerate the vehicle;

You should check idle action as FIRST priority. For change lane action, CAREFULLY CHECK the safety of vehicles on target lane. Consider acceleration action carefully. The deceleration action is LAST priority.

To check decision safety you should follow steps:

Step 1: Get the vehicles in this lane that you may affect. Acceleration, deceleration and idle action affect the current lane, while left and right lane changes affect the corresponding lane.

Step 2: If there are vehicles, check safety between ego and all vehicles in the action lane ONE by ONE.

Remember to use the proper tools mentioned in the tool list ONCE a time.

Thought: Given the current scenario and the rules for making a decision, the first step is to understand the state of the 'ego' car and its surroundings. The 'ego' car is currently in lane 1, with a speed of 16.7. There are vehicles in front (veh7 and veh12) and behind (no specific vehicle mentioned behind in lane 1) in the same lane, and vehicles in adjacent lanes that could affect decision-making for lane changes.

To make an informed decision, I need to first understand the available lanes for the 'ego' car to ensure any lane change decision is based on the current lane configuration.

Observation: The available lane of ego is lane_1, lane_2 and lane_0. lane_1 is the current lane. lane_2 is to the right of the current lane. lane_0 is to the left of the current lane.

Thought: With the available lanes identified as lane_0 to the left, lane_1 as the current lane, and lane_2 to the right, the next step is to assess the current traffic situation in these lanes to make a safe and informed decision. Given the rules and attention points, it's crucial to first consider the idle action to see if maintaining the current speed and lane is a viable and safe option. This requires understanding the vehicles in the current lane (lane_1) that may affect this decision.

Observation:

veh7 is driving at 18.1m/s on lane_1, and it's driving in front of ego car for 40.0099983215332 meters. You need to make sure that your actions do not conflict with each of the vehicles mentioned.

Thought:

Given the observation that vehicle 7 (veh7) is ahead of the ego car in lane 1 with a speed of 18.1 m/s and is 40.01 meters ahead, it's important to consider the safety and rules for making a decision. Since veh7 is moving faster than the ego car (16.7 m/s), maintaining the current speed (idle action) could be a viable option as it would not decrease the distance between the ego car and veh7 rapidly, adhering to the rule of keeping a safe distance. However, to ensure this decision is safe and in line with the guidelines provided, I need to check if keeping the current speed (idle) is safe considering the vehicle ahead in the same lane.

Action:

```
{
  "action": "Is Keep Speed Conflict With Car",
  "action_input": "veh7"
}
```

Observation:

keep lane with current speed is safe with veh7

Thought:

agent finished

Given that maintaining the current speed (idle action) is safe with respect to veh7, which is ahead of the ego car in lane 1, and considering the rules and attention points provided, it seems that the best decision for the ego car at this moment is to remain in its current lane at its current speed. This decision adheres to the principle of keeping a safe distance from the car in front, as well as the guidance to prioritize the idle action when safe to do so. Additionally, this choice respects the rule against frequent lane changes, ensuring that the ego car's driving behavior remains predictable and safe for surrounding traffic.

Final Answer:

```
{
  "decision": "IDLE",
  "explanations": "Maintaining the current speed and lane is chosen to ensure safety by keeping a safe distance from the vehicle ahead (veh7) and adhering to the rules against frequent lane changes. This decision is based on the current traffic scenario and the rules provided for safe and responsible driving on the highway."
}
```

Figure 11: Interaction between the LLM-based agent and the HighwayEnv environment.